Membrane Orientation of MSI-78 Measured by Sum Frequency Generation Vibrational Spectroscopy

ARTICLE *in* LANGMUIR · JUNE 2011

Impact Factor: 4.46 · DOI: 10.1021/la201048t · Source: PubMed

3 AUTHORS, INCLUDING:

Pei Yang
University of Michigan
23 PUBLICATIONS **296** CITATIONS
SEE PROFILE

Ayyalusamy Ramamoorthy
University of Michigan
336 PUBLICATIONS **11,737** CITATIONS
SEE PROFILE

Langmuir

ARTICLE

pubs.acs.org/Langmuir

Membrane Orientation of MSI-78 Measured by Sum Frequency Generation Vibrational Spectroscopy

Pei Yang, Ayyalusamy Ramamoorthy, and Zhan Chen*

Biophysics and Department of Chemistry, 930 North University Avenue, University of Michigan, Ann Arbor, Michigan 48109, United States

ABSTRACT: Antimicrobial peptides (AMPs) selectively disrupt bacterial cell membranes to kill bacteria whereas they either do not or weakly interact with mammalian cells. The orientations of AMPs in lipid bilayers mimicking bacterial and mammalian cell membranes are related to their antimicrobial activity and selectivity. To understand the role of AMP−lipid interactions in the functional properties of AMPs better, we determined the membrane orientation of an AMP (MSI-78 or pexiganan) in various model membranes using sum frequency generation (SFG) vibrational spectroscopy. A solid-supported single 1,2-dipalmitoyl-*an*-glycero-3-[phospho-*rac*-(1-glycerol)] (DPPG) bilayer or 1-palmitoyl-2-oleoyl-*sn*-glycero-3-[phospho-*rac*-(1-glycerol)] (POPG) bilayer was used as a model bacterial cell membrane. A supported 1,2-dipalmitoyl-*an*-glycero-3-phosphocholine (DPPC) bilayer or a 1-palmitoyl-2-oleoyl-*sn*-glycero-3-phosphocholine (POPC) bilayer was used as a model mammalian cell membrane. Our SFG results indicate that the helical MSI-78 molecules are associated with the bilayer surface with ∼70° deviation from the bilayer normal in the negatively charged gel-phase DPPG bilayer at 400 nM peptide concentration. However, when the concentration was increased to 600 nM, MSI-78 molecules changed their orientation to make a 25° tilt from the lipid bilayer normal whereas multiple orientations were observed for an even higher peptide concentration in agreement with toroidal-type pore formation as reported in a previous solid-state NMR study. In contrary, no interaction between MSI-78 and a zwitterionic DPPC bilayer was observed even at a much higher peptide concentration (∼12 000 nM). These results demonstrate that SFG can provide insights into the antibacterial activity and selectivity of MSI-78. Interestingly, the peptide exhibits a concentration-dependent membrane orientation in the lamellar-phase POPG bilayer and was also found to induce toroidal-type pore formation. The deduced lipid flip-flop from SFG signals observed from lipids also supports MSI-78-induced toroidal-type pore formation.

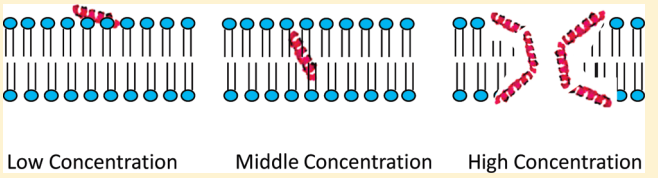

1. INTRODUCTION

Various peptides have been designed and tested as antimicrobial compounds to prevent bacterial drug resistance.[1,2] It has been widely shown that antimicrobial peptides (AMPs) can differentiate mammalian cell membranes from bacteria cell membranes and selectively kill bacteria without harming mammalian cells.[3−7] An ideal AMP should have high efficacy in killing bacterial cells and no hemolytic activity. An examination of the detailed structural information of AMPs associated with various cell membranes can lead to a further understanding of peptide−membrane interactions, aiding in the design and development of AMPs with improved properties. Bacterial cell membranes contain ∼25% negatively charged lipids, and a mammalian cell membrane usually consists of zwitterionic lipids such as phosphatidylcholine (PC). The electrostatic attraction between negatively charged lipids (such as 1-palmitoyl-2-oleoyl-sn-glycero-3-[phospho-*rac*-(1-glycerol)] or POPG) and a positively charged AMP is believed to be responsible for the binding of AMPs to bacterial cell membranes but not the mammalian ones. To avoid the complexity of the native cell membrane, substrate-supported lipid bilayers have been commonly used as models for the cell membrane.[8−13] In this study, we used such model membranes to investigate AMP−membrane interactions.

Many AMPs kill bacteria by disrupting their cell membranes. Several modes of action of AMPs have been proposed: barrel stave, toroidal pore, carpetlike, and others.[5,7,14−17] In these different modes of action, AMPs adopt different orientations relative to the membrane surface. Therefore, important information regarding the AMP mode of action can be deduced by determining the membrane orientation of an AMP.

Recently, a nonlinear optical spectroscopic technique, sum frequency generation (SFG) vibrational spectroscopy, has been successfully applied to determine the membrane orientation of peptides (including AMPs) and proteins.[18−26] SFG provides the vibrational spectra of surfaces and interfaces with a submonolayer surface specificity.[27−46] It requires only a very small amount of sample and can probe surfaces and interfaces in real time. NMR techniques have been widely used to investigate the molecular interactions between AMPs and model cell membranes, and excellent results have been obtained in such studies.[47−54] Unlike NMR, which uses premixed multilayer lipid−peptide mixtures, SFG can probe interactions between AMPs and a single supported lipid bilayer in situ in real time.

Received: March 20, 2011
Revised: May 9, 2011
Published: May 19, 2011

dx.doi.org/10.1021/la201048t | *Langmuir* 2011, 27, 7760–7767

Scheme 1. (Top to bottom) Molecular Structures of 1,2-Dipalmitoyl-*an*-glycero-3-[phospho-*rac*-(1-glycerol)] (DPPG), 1,2-Dipalmitoyl-*an*-glycero-3-phosphocholine (DPPC), 1-Palmitoyl-2-oleoyl-*sn*-glycero-3-[phospho-*rac*-(1-glycerol)] (POPG), and 1-Palmitoyl-2-oleoyl-*sn*-glycero-3-phosphocholine (POPC)

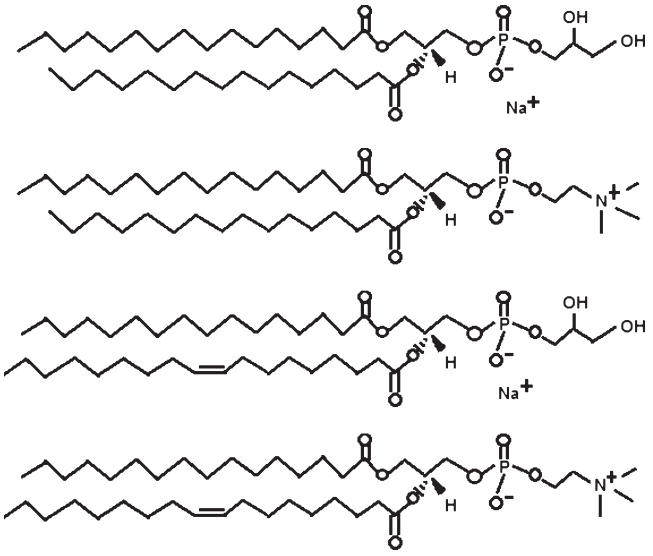

MSI-78 (also known as pexiganan) is a designed synthetic peptide that is an analog of magainin 2 but with a much higher antimicrobial activity and selectivity.[54,55] Previous research on MSI-78 reported that it adopts an α-helical structure in a membrane environment. The orientation of MSI-78 molecules in membranes studied by using various techniques including NMR[54,56−58] revealed that the amphipathic helical peptide is oriented on the surface of the lipid bilayer. Although these results are exciting and provide insights into the function of MSI-78, NMR studies typically require approximately milligram quantities of the peptide. However, there is significant interest in understanding the peptide−membrane interactions at a lower peptide concentration, and experimental data under such conditions are unavailable for MSI-78. For example, experimental measurements from lipid bilayer samples containing a peptide concentration at the minimum inhibitory concentration (MIC) or lower will provide physiologically relevant results.

In this article, we report SFG experimental results on MSI-78 embedded in model bacterial and mammalian cell membranes. We determined the membrane orientations of MSI-78 in various lipid bilayers. Our results further reveal that MSI-78 can strongly interact with model bacterial cell membranes and induce strong disruptions whereas it could not disrupt model mammalian cell membranes at similar peptide concentrations.

2. MATERIALS AND METHODS

2.1. Materials. MSI-78 is a 22-residue synthetic α-helical peptide (amino acid sequence G-I-G-K-F-L-K-K-A-K-K-F-G-K-A-F-V-K-I-L-K-K-NH_2) and was synthesized and purified using the standard method.[54] Different lipids were purchased from Avanti Polar Lipids (Alabaster, AL), including 1,2-dipalmitoyl-*an*-glycero-3-[phospho-*rac*-(1-glycerol)] (DPPG), 1,2-dipalmitoyl-d_{62}-*sn*-glycero-3-[phospho-*rac*-(1-glycerol)] (*d*-DPPG), 1,2-dipalmitoyl-*an*-glycero-3-phosphocholine (DPPC), 1-palmitoyl-2-oleoyl-*sn*-glycero-3-[phospho-*rac*-(1-glycerol)] (POPG), and 1-palmitoyl-2-oleoyl-*sn*-glycero-3-phosphocholine (POPC). The molecular structures of the lipids are shown in Scheme 1. Right-angle CaF_2 prisms were purchased from Altos (Trabuco Canyon, CA). The CaF_2 prisms were soaked in toluene for 1 day and then sonicated in Contrex AP solution from Decon Laboratories (King of Prussia, PA) for 1 h. After that, they were cleaned in methanol for 10 min and then rinsed thoroughly with deionized water. The prisms were treated in a glow discharge plasma chamber for 4 min immediately before the deposition of lipids. The Langmuir−Blodgett and Langmuir−Schaefer (LB/LS) methods were used to deposit the proximal and the distal leaflets of a single lipid bilayer onto the prisms, respectively. A KSV2000 LB system and ultrapure water from a Millipore system (Millipore, Bedford, MA) were used throughout the experiments for bilayer preparation, as described previously.[18] In our experiments, we used negatively charged DPPG/*d*-DPPG or POPG/POPG bilayers to represent bacterial cell membranes. Zwitterionic DPPC/DPPC or POPC/POPC bilayers were used to model mammalian cell membranes for comparison. The transition temperature between the gel and fluid phases for POPG or POPC lipid is −2 °C whereas that for DPPG (*d*-DPPG) or DPPC lipid is 41 °C. All of the experiments were carried out at room temperature (~24 °C), at which the DPPG/*d*-DPPG and DPPC/DPPC bilayers are in the gel phase and the POPG/POPG and POPC/POPC bilayers are in the fluid phase. In peptide−lipid bilayer interaction experiments, an appropriate amount of MSI-78 aqueous stock solution was injected into a reservoir filled with 2 mL of ultrapure water (in contact with the supported lipid bilayer) to achieve the desired peptide solution concentration. The SFG spectra were then collected after the peptide−lipid bilayer interaction reached equilibrium and the SFG signal became stable (around 1 h after the injection of the peptide solution into the subphase of the lipid bilayer). A magnetic microstirrer was used to ensure a homogeneous concentration distribution of MSI-78 in the subphase below the lipid bilayer.

2.2. SFG. SFG is a second-order nonlinear optical spectroscopic technique that has submonolayer surface sensitivity. The details regarding SFG theories and measurements have been published previously[27−46] and will not be repeated here. The SFG setup used in this study was purchased from EKSPLA. In our experiments here, two laser beams (a 532 nm visible and a frequency-tunable infrared) are overlapped in space and time on the sample, generating a signal at the sum frequency ($\omega_{vis} + \omega_{IR} = \omega_{sum}$). The pulse energies of both input beams are around 100 μJ, and the beam sizes are around 500 μm. By controlling the polarization of the input and generated signal beams, information on the interfacial molecular orientation can be obtained. All of the spectra presented in this article were collected using nearly total internal reflection geometry[59] with ssp (an s-polarized output SFG signal, s-polarized input visible beam, and p-polarized input IR beam, respectively) and ppp polarization combinations with 100 shots for each data point. For peptide amide I spectra, at least five same spectra were collected and averaged for data analysis.

The AMP conformation can be deduced from the peak center of the SFG amide I signal. For an α-helical structure, the amide I signal is centered at about 1650 cm^{-1}.[60] The orientation of an α-helical peptide can be determined by using SFG amide I spectra collected with ssp and ppp polarization combinations.[18,61] This method has been applied to examine the membrane orientation of α-helical structures such as magainin 2,[18] alamethicin,[23] melittin,[20] cytochrome b5,[26] and G protein.[25]

3. RESULTS AND DISCUSSION

3.1. MSI-78 in a DPPG/*d*-DPPG Lipid Bilayer. After the MSI-78 stock solution was injected into the subphase of the DPPG/*d*-DPPG (DPPG as the proximal leaflet and *d*-DPPG as the distal leaflet) bilayer, the SFG signal at 1650 cm^{-1} was monitored as a function of time. At a peptide concentration of 300 nM, no discernible SFG signal was detected in the amide I frequency

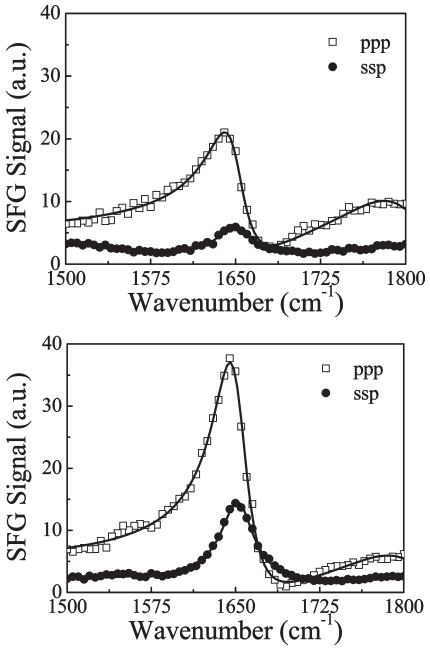

Figure 1. SFG ppp and ssp amide I spectra collected from a DPPG/*d*-DPPG bilayer in contact with a (top) 400 nM or (bottom) 600 nM MSI-78 solution.

region. This can be explained by the fact that the interaction between MSI-78 molecules and the DPPG/*d*-DPPG bilayer could be very weak at this low peptide concentration. For higher concentrations, the SFG signal at 1650 cm^{-1} was detected and reached equilibrium about 1 h after the peptide injection into the subphase. SFG ppp and ssp spectra of MSI-78 in a DPPG/*d*-DPPG bilayer were then collected. Figure 1 shows the spectra collected after a 400 (top) or 600 nM (bottom) MSI-78 solution was placed in contact with the DPPG/*d*-DPPG bilayer (after 1 h). In Figure 1, all amide I SFG spectra exhibit a dominant peak centered at 1650 cm^{-1}, indicating that MSI-78 adopts an α-helical structure associated with a DPPG/*d*-DPPG bilayer.[60] The solid lines in Figure 1 are the fitting results. Details of the SFG peak fitting methods have been described in previous publications[18] and will not be reiterated here. According to the fitting results, we obtained the measured ppp and ssp signal strength ratio (or χ_{ppp}/χ_{ssp}) of 2.0 for 400 nM or 1.5 for 600 nM MSI-78 solution. By using this ratio, we can determine the orientation angle of MSI-78 in the DPPG/*d*-DPPG bilayer.

SFG orientation analysis for an α-helical structure has been described in our previous publications.[18,61] We defined that orientation angle θ represents the tilt angle between the principal axis of the α-helical MSI-78 molecule and the DPPG/*d*-DPPG bilayer surface normal. The relation between the measured χ_{ppp}/χ_{ssp} ratio of MSI-78 and α-helix orientation angle θ can be deduced using the developed method, assuming a δ-orientation distribution (Figure 2).[61] Using Figure 2 and the measured χ_{ppp}/χ_{ssp} ratios, we deduced that the orientation angle θ of MSI-78 associated with the DPPG/*d*-DPPG bilayer is around 70° (or 25°) when the bilayer is in contact with the 400 (or 600) nM MSI-78 solution. Other concentrations of MSI solutions were also tested in the experiment. As shown in Figure 2, when the MSI-78 solution concentration increased, the tilt angle θ decreases, meaning that the orientation of MSI-78 molecules changes from surface orientation to transmembrane in the

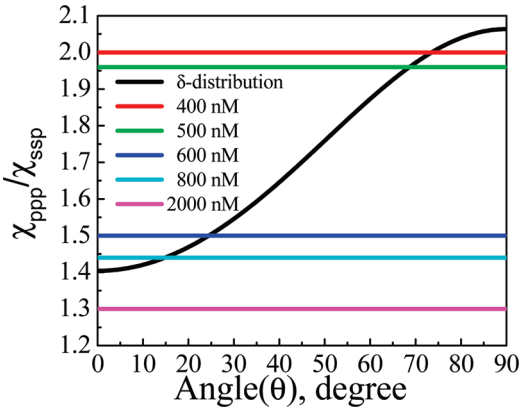

Figure 2. Relation between the χ_{ppp}/χ_{ssp} ratio and the orientation angle of MSI-78 molecules in a DPPG/*d*-DPPG bilayer.

DPPG/*d*-DPPG bilayer. At 400 nM, MSI-78 molecules are tilted 70° from the bilayer normal. At a peptide concentration of 500 nM, the orientation angle changed from 70 to 65°. When the peptide concentration was increased to 600 nM, the orientation angle changed to 25°, which is close to the transmembrane orientation. This shows that the increase in the peptide concentration enables the MSI-78 molecules to change their orientation from perpendicular to the DPPG/*d*-DPPG bilayer normal to the parallel orientation. As the concentration continued to increase to 800 nM, the orientation angle of MSI-78 molecules was determined to be approximately 15° versus the bilayer normal. At an even higher concentration of 2000 nM, the measured χ_{ppp}/χ_{ssp} ratio equals 1.3, which is below the possible values in the calculated curve assuming a δ-orientation distribution (Figure 2). Under the assumption that every MSI-78 molecule adopts the same orientation (or a δ-orientation distribution), the value of χ_{ppp}/χ_{ssp} should be between 1.40 and 2.05. The observation of a low peptide concentration is in excellent agreement with previous solid-state NMR studies[54] whereas the change in the tilt angle at higher concentrations (500 to 800 nM) indicates that the peptide could be aggregating to insert into the hydrophobic region of the bilayer. Such transmembrane orientations were not observed from NMR experiments;[58] therefore, we believe that there are two different mechanisms in operation for low ($<\mu$M) and high concentrations of the peptide.

Previously, when we used SFG to investigate the orientation of melittin molecules in a DPPG/DPPG bilayer,[20] we observed the same phenomenon and found that the measured χ_{ppp}/χ_{ssp} value was below the possible values of χ_{ppp}/χ_{ssp} assuming a δ-orientation distribution for melittin. The combined SFG and ATR-FTIR study showed that melittin molecules associated with the lipid bilayer adopt two distinct orientations: about a quarter of the melittin molecules orient almost perpendicularly inside the lipid bilayer whereas the rest orient almost parallel to the bilayer surface.[20] Here we believe that for MSI-78, when the peptide concentration reaches 2000 nM, the MSI-78 molecules also adopt multiple orientations. This interpretation is similar to the solid-state NMR observation in which MSI-78 functions via toroidal-pore formation, where the peptide exists in multiple orientations.[54] This observation is also consistent with the membrane thinning effect observed from AFM experiments.[56] In addition, it is also possible that some of the lipids may be removed by the peptide (like a detergent), as revealed by the

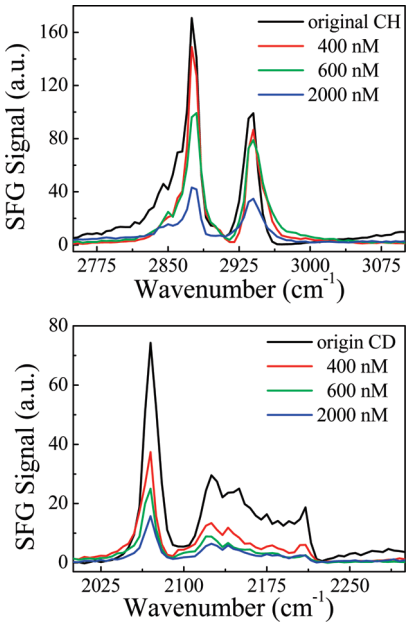

Figure 3. SFG ssp spectra of the (top) C−H and (bottom) C−D stretching frequency ranges collected from a DPPG/*d*-DPPG bilayer before and after contact with MSI-78 solutions with three different solution concentrations.

observation of isotropic chemical shift peaks in some samples for solid-state NMR.[58] Then some peptides may tilt or lie down on the bare CaF_2 substrate surface.

It has been shown in previous studies that the MIC of MSI-78 against *E. coli* is around 5 μM.[55,62,63] In our experiment, the membrane insertion observed for concentrations <1 μM may not result in bilayer disruption but the multiple orientations observed at a higher concentration (2 μM) could result in bilayer disruption via toroidal-type pore formation. Though the MIC is still higher than 2 μM, it is reasonable because the *E. coli* cell membrane contains only about 32% anionic lipids, thus requiring a higher peptide concentration to disrupt the cell membrane as revealed by the MIC value.

MSI-78 is a magainin 2 analog but has different antimicrobial activity and selectivity.[55,62,63] In our previous research, we investigated the molecular interactions between magainin 2 and different model cell membranes such as POPG/POPG and POPC/POPC bilayers.[18] Similar results were observed for magainin 2 compared to those for MSI-78. At a low concentration of 200 nM, no SFG signal can be observed, indicating that magainin 2 molecules either do not interact with the bilayer or lie down on the bilayer surface.[18] After increasing the magainin 2 concentration to 800 nM, the magainin 2 molecules insert into the POPG lipid bilayer and adopt a transmembrane orientation with an orientation angle of 20° from the bilayer normal.[18]

Different modes of AMP action on lipid bilayers will result in different lipid bilayer changes and time-dependent changes, which in turn will correspond to different SFG spectral features and spectral changes as a function of time. In our experiment, we used an isotopically asymmetric DPPG/*d*-DPPG (DPPG as the proximal leaflet and *d*-DPPG as the distal leaflet) bilayer. Therefore, we could specifically monitor the proximal and distal leaflets separately if we assume that no flip-flop occurred. The behavior

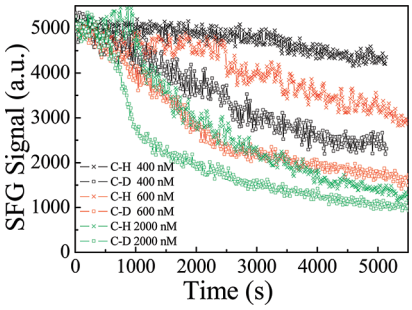

Figure 4. Time-dependent SFG spectral intensity monitored at 2875 cm^{-1} (for the proximal methyl C−H symmetric stretching mode) and at 2070 cm^{-1} (for the distal methyl C−D symmetric stretching mode). The MSI-78 solution was injected at 200 s.

of each leaflet of the bilayer was monitored by examining the SFG spectra collected in the C−H stretching frequency regime (2750−3100 cm^{-1}) and the C−D stretching frequency regime (2000−2300 cm^{-1}). Figure 3 shows the SFG spectra (ssp) in the (top) C−H and (bottom) C−D stretching frequency ranges collected from a DPPG/*d*-DPPG bilayer before and after being placed in contact with MSI-78 solutions with different concentrations. MSI-78 contains some C−H groups, but their signals are much weaker than those from the DPPG leaflet. Therefore, it is believed that the SFG C−H stretching signal is attributed to the proximal leaflet (DPPG) and the SFG C−D stretching signal comes from the distal leaflet (*d*-DPPG).

As displayed in Figure 3, the overall SFG spectral intensity in the C−D stretching region dramatically decreased at a peptide concentration of 400 nM, whereas the SFG intensity in the C−H stretching region changed only slightly. As we showed above from SFG studies on the peptide amide I signals, MSI-78 tilts to about 70° in the bilayer. Therefore, MSI-78 may interact only with the distal leaflet and disrupt some order of the distal leaflet peptide chain. The C−D signals are dominated by the contributions from the end CD_3 groups of the distal leaflet. The orientations of such CD_3 groups must change substantially even when the peptide solution concentration is 400 nM when MSI-78 interacts only with the distal leaflet. Because the peptide does not interact with the proximal leaflet significantly, no large change in the CH signals was observed.

At a peptide concentration of 600 nM, both the SFG C−D and C−H signal intensities decreased substantially, indicating that both the distal and proximal leaflets in the DPPG/*d*-DPPG bilayer were disrupted at this peptide concentration. According to the above SFG amide I signals, at this concentration MSI-78 adopts a transmembrane orientation, which apparently can disrupt both leaflets. As in the 400 nM study above, here SFG studies on the C−H and C−D stretching frequencies are well correlated to the SFG amide I signals reported above. At a high peptide concentration of 2000 nM, the SFG C−D and C−H stretching signals are very weak, showing that the lipid bilayer must be severely disrupted. In this situation, MSI-78 molecules form toroidal pores inducing the flip-flop of lipids, and there could be some removal of lipids via the detergent-type interaction of the peptide with the bilayer.

We also followed the kinetics during the process when MSI-78 molecules interact with the DPPG/*d*-DPPG bilayers at different peptide concentrations. Such kinetics can be monitored by detecting SFG C−H and C−D stretching signal intensity

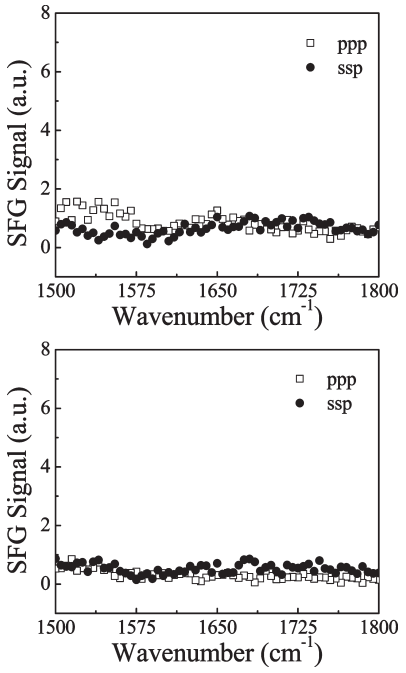

Figure 5. SFG ppp and ssp amide I spectra collected from a DPPC/DPPC bilayer in contact with a (top) 6000 or (bottom) 12 000 nM MSI-78 solution. No discernible signal was observed.

changes as a function of time. Time-dependent SFG signals were monitored at 2875 cm^{-1} for the CH_3 symmetric stretching mode from the proximal leaflet (DPPG) and at 2070 cm^{-1} for the CD_3 symmetric stretching mode from the distal leaflet (*d*-DPPG). A signal decrease at 2875 or 2070 cm^{-1} would indicate the perturbation (or disruption) in the proximal (DPPG) or the distal (*d*-DPPG) leaflet, respectively, or the reduction of the asymmetry of the lipid bilayer induced by peptide insertion. Figure 4 shows such time-dependent signal changes at three different peptide solution concentrations whereas the MSI-78 stock solutions with different concentrations were injected at 200 s into the lipid subphase.

Figure 4 shows that after the 400 nM peptide solution was introduced, both SFG C−D and C−H stretching intensities started to decrease but to very different extents. The C−D stretching signal, which was contributed by the distal leaflet (*d*-DPPG), was reduced much faster than the C−H stretching signal (from the proximal leaflet, DPPG). This result is again well correlated with the above observation. Because MSI-78 molecules tilt only slightly on the bilayer surface, they disrupted the distal leaflet first and significantly but did not disrupt with the proximate leaflet substantially. The SFG signal from the proximal leaflet changed only slightly because MSI-78 molecules do not interact with the proximal leaflet very much. When the peptide concentration increases to 600 nM, in addition to the substantial SFG C−D stretching signal intensity decrease, the SFG C−H stretching signal also decreased greatly, indicating that both the distal (*d*-DPPG) and proximal (DPPG) leaflets were disrupted at this concentration. This agrees with the observation that the MSI-78 molecules adopt a transmembrane orientation in the DPPG/*d*-DPPG bilayer. At an even higher concentration of 2000 nM, both C−D and C−H stretching signals decreased quickly, showing that both the distal and the proximal leaflets were disrupted rapidly at this high concentration, along with the

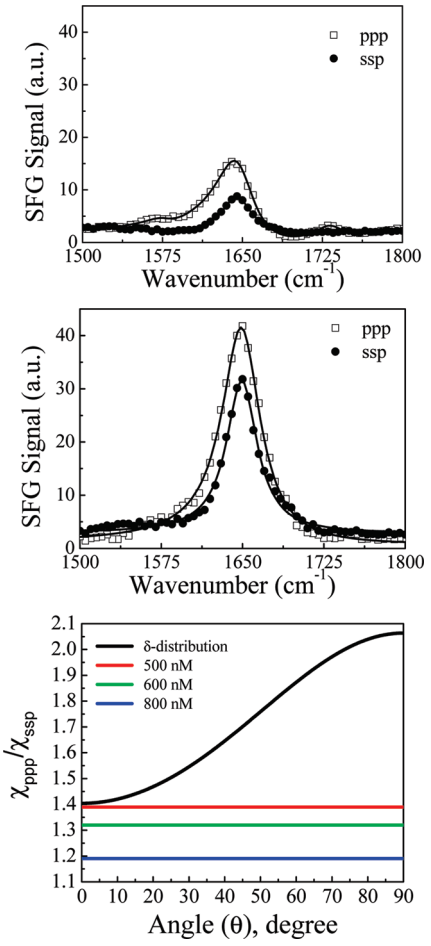

Figure 6. SFG ppp and ssp amide I spectra collected from a POPG/POPG bilayer in contact with a (top) 500 or (middle) 800 nM MSI-78 solution. (Bottom) Relation between the χ_{ppp}/χ_{ssp} ratio and the orientation angle of MSI-78 in a POPG/POPG bilayer.

possible flip-flop. The time-dependent studies here further confirm the different interactions between MSI-78 and the DPPG bilayer at different peptide concentrations.

3.2. MSI-78 in a DPPC/DPPC Lipid Bilayer. After we studied the interactions between MSI-78 and DPPG bilayers (models for bacterial cell membranes), we continued to study the interactions between MS-78 and DPPC bilayers (models for mammalian cell membranes). The SFG ppp and ssp spectra of MSI-78 associated with DPPC/DPPC bilayers are shown in Figure 5. The spectra were collected after 6000 (top) or 12 000 nM (bottom) MSI-78 solutions were placed in contact with the DPPC/DPPC bilayer. As shown in Figure 5, there was no discernible SFG signal detected in the amide I frequency region at peptide concentrations of 6000 and 12 000 nM. This can be explained by the fact that the MSI-78 molecules do not interact and are not associated with the DPPC/DPPC bilayer. The concentration that we used here (12 000 nM) is 30 times larger than that in the DPPG/*d*-DPPG bilayer study (400 nM), but still no MSI-78 molecules interact with the DPPC/DPPC bilayer. It is thus obvious that the interaction between MSI-78 and the DPPC/DPPC bilayer is very weak, which is quite different from the interaction between MSI-78 and the negatively charged DPPG/*d*-DPPG bilayer. Because DPPC is a zwitterionic lipid, positively charged MSI-78 cannot be attracted to the DPPC/DPPC bilayer because of

dx.doi.org/10.1021/la201048t |*Langmuir* 2011, 27, 7760–7767

the lack of electrostatic interaction. We can conclude that there is no observed interaction between MSI-78 and the model mammalian cell membrane. This can explain the excellent selectivity of MSI-78.

3.3. MSI-78 in a POPG/POPG Lipid Bilayer. POPG/POPG and POPC/POPC bilayers were used as models for bacterial and mammalian cell membranes in our previous SFG studies on magainin 2.[18] Here, we also used an anionic POPG/POPG bilayer to represent the bacterial cell membrane. We studied the interactions between MSI-78 and the POPG/POPG bilayer for two reasons: First, different from the gel-phase DPPG/*d*-DPPG bilayer, the POPG/POPG bilayer is in the fluid phase at room temperature. The real cell membrane is in the fluid phase; therefore, fluid-phase POPG/POPG should better represent the bacterial cell membrane compared to the DPPG/*d*-DPPG bilayer. Second, as shown in our previous paper, some peptides such as alamethicin interact with gel- and fluid-phase lipid bilayers differently.[23] It was shown that alamethicin molecules lie down or aggregate on the gel-phase lipid bilayer surface but can insert into the fluid-phase lipid bilayer.[23] Therefore, the use of lipids with different phases in the study should provide a more complete picture of MSI-78/cell membrane interactions.

SFG ppp and ssp spectra of MSI-78 in a POPG/POPG bilayer were collected as described above (Figure 6). The spectra were collected after the POPG/POPG bilayer was placed in contact with MSI-78 solutions with concentrations of 500 (top) and 800 nM (middle). At a lower peptide concentration of 400 nM, no discernible SFG signal in the amide I region could be detected from the POPG/POPG bilayer/peptide solution interface (data not shown). This can be explained by the fact that the interaction between MSI-78 and the POPG/POPG bilayer was very weak at such a low peptide concentration. At a concentration of 500 nM, both SFG ssp and ppp spectra exhibit a dominant peak centered at around ~1650 cm^{-1}, which confirms that MSI-78 adopted an α-helical structure in the fluid-phase POPG/POPG bilayer (similar to that in the gel-phase DPPG bilayer above).[60] The weak signal at about 1730 cm^{-1} in the ppp spectrum for 500 nM is from the lipid bilayer, not the peptide.

The fitted experimental signal strength ratio of χ_{ppp}/χ_{ssp} for the ~1650 cm^{-1} peak equals 1.39 and 1.19 for 500 and 800 nM MSI-78 solutions, respectively. Figure 6 (bottom) displays the relationship between the measured χ_{ppp}/χ_{ssp} ratio and orientation angle θ for MSI-78 molecules. At a concentration of 500 nM, the tilt angle between the principal axis of MSI-78 molecules and the POPG/POPG bilayer surface normal is around 0°, indicating that MSI-78 molecules insert into the POPG/POPG bilayer and adopt a transmembrane orientation at this concentration. When the MSI-78 solution concentration is increased to 600 or 800 nM, the measured ratio of χ_{ppp}/χ_{ssp} is below the calculated curve (assuming a δ-orientation distribution) in Figure 6, showing that MSI-78 molecules may have more than one distinct orientation —under these conditions, the toroidal pores are formed as discussed earlier. Also, the lipid bilayer might be severely disrupted as discussed above. At a concentration of 500 nM, it is sufficient for MSI-78 molecules to interact effectively with the lamellar-phase POPG/POPG bilayer, so these peptides adopt a transmembrane orientation. Our previous gel-phase DPPG/*d*-DPPG bilayer results indicate that such a concentration for the DPPG bilayer is around 600 nM, which is similar to the fluid-phase POPG/POPG bilayer result (500 nM).

The orientation angle at 0° may not be the only possible solution for 500 nM. Possibly, at this concentration peptides have already started to adopt multiple orientations, which may also satisfy the experimental signal strength ratio of χ_{ppp}/χ_{ssp} = 1.39. To quantify the orientation further, we will include more measurements in the experiment.[20]

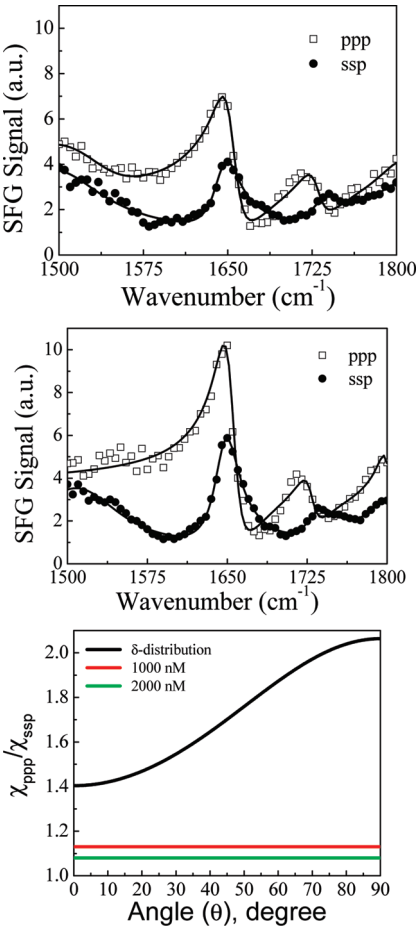

Figure 7. SFG ppp and ssp amide I spectra collected from a POPC/POPC bilayer in contact with a (top) 1000 or (middle) 2000 nM MSI-78 solution. (Bottom) Relation between the χ_{ppp}/χ_{ssp} ratio and the orientation angle of MSI-78 in a POPC/POPC bilayer. The signals at 1725 cm^{-1} are due to the lipid molecules.

3.4. MSI-78 in a POPC/POPC Lipid Bilayer. Last, we used the fluid-phase POPC/POPC bilayer as a representation of the model mammalian cell membrane. Different from the negatively charged POPG lipid, POPC is a zwitterionic lipid. The SFG ppp and ssp spectra of MSI-78 molecules in a POPC/POPC bilayer are shown in Figure 7. The spectra were collected after 1000 (top) or 2000 nM (middle) MSI-78 solution was placed in contact with the POPC/POPC bilayer. Different from the POPG result, at a concentration of 800 nM, no discernible SFG signal in the amide I region could be detected (data not shown), which shows that the MSI-78 molecules do not bind to the POPC/POPC bilayer, the MSI-78 coverage on the POPC/POPC bilayer is not high enough, or the MSI-78 molecules completely lie down on the bilayer surface. By increasing the MSI-78 concentration to 1000 nM, we observed a very weak SFG signal (intensity around 7 in the SFG ppp spectra) in the amide I frequency region, showing that perhaps a small number of peptides were associated with the POPC/POPC bilayer at this concentration. This observation is different from the gel-phase

dx.doi.org/10.1021/la201048t |*Langmuir* 2011, 27, 7760–7767

DPPC/DPPC bilayer result. For the DPPC bilayer, as we showed in Figure 5, no detectable SFG signal was observed even at a much higher MSI-78 concentration of 12 000 nM, indicating that there is no interaction between MSI-78 and the DPPC/DPPC bilayer. Here, we believe that the weak SFG signal from MSI-78 in the fluid-phase POPC/POPC bilayer may be due to a small number of MSI-78 peptides associated with the bilayer. The fitted experimental signal strength ratios of χ_{ppp}/χ_{ssp} at the peak center of ~1650 cm^{-1} are 1.13 and 1.08 for 1000 and 2000 nM peptide solutions, respectively. Figure 7 (bottom) again shows the relationship between the measured χ_{ppp}/χ_{ssp} ratio and orientation angle θ for MSI-78 molecules. At a concentration of 1000 or 2000 nM, the measured ratio of χ_{ppp}/χ_{ssp} is below the calculated curve, assuming a δ-orientation distribution in Figure 7. Thus, MSI-78 molecules again have more than one distinct orientation, suggesting that the lipid-bound peptides induce toroidal-type pore formation.

Although we observed the SFG amide I signals from MSI-78 in both POPG/POPG and POPC/POPC bilayers, the interactions between MSI-78 molecules and the two lipid bilayers are very different: (1) The SFG intensities of MSI-78 with the two lipid bilayers are very different. The SFG intensity detected from MSI-78 associated with the POPG/POPG bilayer is about 16 (intensity counts) at a peptide concentration of 500 nM. The SFG intensity of MSI-78 in the POPC/POPC bilayer is much weaker, only about 7 (intensity counts) at a much higher peptide concentration of 1000 nM. Even if we double this concentration to 2000 nM, the SFG intensity from MSI-78 in the POPC/POPC bilayer is still much weaker than that in the POPG/POPG bilayer at a low peptide concentration of 500 nM. (2) The orientation angle of MSI-78 molecules should be very different in these two kinds of lipid bilayers. For the POPG/POPG bilayer, the MSI-78 molecules insert into the membrane bilayer at a peptide concentration of 500 nM with a measured orientation angle of 0° versus the surface normal. After increasing the peptide concentration to 600 or 800 nM, toroidal pores may be formed, generating multiple peptide orientations. Also, the lipid bilayer may be severely disrupted or demolished and the peptide molecules could adopt dual δ-function orientations. However, MSI-78 molecules with one distinct orientation in the POPC/POPC bilayer were never observed at any peptide concentration because of the lack of electrostatic attraction between MSI-78 and the zwitterionic lipid bilayer. This could be because the hydrophobic interaction dominates above a certain peptide concentration, enabling multiple orientations directly via toroidal-type pore disruption. Thus, the observed differences in the interactions between MSI-78 and anionic POPG/POPG versus zwitteroinic POPC/POPC bilayers show clear evidence that MSI-78 interacts with bacterial cell membranes and mammalian cell membranes quite differently.

4. CONCLUSIONS

In this article, the orientation angles of MSI-78 molecules in different model membrane environments have been measured using SFG amide I spectra detected with different polarization combinations. The SFG orientation analysis on α-helical structures used here is based on a methodology developed previously in our laboratory. We compared the orientations of MSI-78 molecules in both model bacterial (DPPG or POPG) and mammalian (DPPC or POPC) cell membranes. For a gel-phase DPPG/*d*-DPPG bilayer at a low peptide concentration of 400 nM, MSI-78 molecules were oriented on the surface of a lipid bilayer as reported from solid-state NMR studies.[54] When the peptide concentration is increased to 600 nM, MSI-78 molecules insert into the lipid bilayer. Heterogeneous membrane orientations observed at a higher peptide concentration are also in complete agreement with solid-state NMR studies[58] that revealed the formation of toroidal pores due to MSI-78 interaction with lipid bilayers. In contrary, there is no interaction between MSI-78 and the zwitterionic gel-phase DPPC/DPPC bilayer even at a much higher peptide concentration of 12 000 nM. For the fluid lamellar-phase POPG/POPG bilayer, the lipid bilayer could be disrupted at a peptide concentration of 500 nM whereas the MSI-78 molecules insert into the lipid bilayer and eventually disrupt the bilayer via toroidal pores. For the POPC/POPC bilayer, there is no interaction between MSI-78 and the lipid bilayer below a peptide concentration of 1000 nM. These results demonstrate that MSI-78 molecules can easily interact with (or disrupt) the bacterial model cell membranes (DPPG or POPG bilayer), but the disruption of the mammalian model cell membranes (DPPC or POPC bilayer) is much more difficult. Finally, we believe that SFG measurements at a very low peptide concentration (very close to or below the MIC value) can provide fundamental insights into the function of an antimicrobial peptide.

AUTHOR INFORMATION

Corresponding Author

*Fax: 734-647-4865. E-mail: zhanc@umich.edu.

ACKNOWLEDGMENT

This work was supported by the National Institutes of Health (GM081655). We thank Dr. Sathiah Thennarasu for help with this study.

REFERENCES

(1) Zasloff, M. *Nature* **2002**, *415*, 389.
(2) Ding, J. L.; Ho, B. *Drug Dev. Res.* **2004**, *62*, 317.
(3) Matsuzaki, K. *Biochim. Biophys. Acta* **1999**, *1462*, 1.
(4) Hancock, R. E.; Diamond, G. *Trends Microbiol.* **2000**, *8*, 402.
(5) Epand, R. M.; Vogel, H. J. *Biochim. Biophys. Acta* **1999**, *1462*, 11.
(6) Sitaram, N.; Nagaraj, R. *Biochim. Biophys. Acta* **1999**, *1462*, 29.
(7) Brogden, K. A. *Nat. Rev. Microbiol.* **2005**, *3*, 238.
(8) Brian, A. A.; McConnell, H. M. *Proc. Natl. Acad. Sci. U.S.A.* **1984**, *81*, 6159.
(9) Tamm, L. K.; Mcconnell, H. M. *Biophys. J.* **1985**, *47*, 105.
(10) Castellana, E. T.; Cremer, P. S. *Surf. Sci. Rep.* **2006**, *61*, 429.
(11) Chan, Y. H.; Boxer, S. G. *Curr. Opin. Chem. Biol.* **2007**, *11*, 581.
(12) Tamm, L. K.; Graves, J. T. *J. Struct. Biol.* **2009**, *168*, 1.
(13) Liu, J.; Conboy, J. C. *J. Phys. Chem. C* **2007**, *111*, 8988.
(14) Shai, Y. *Biopolymers* **2002**, *66*, 236–248.
(15) Huang, H. W. *Biochemistry* **2000**, *39*, 8347–8352.
(16) Yang, L.; Harroun, T. A.; Weiss, T. M.; Ding, L.; Huang, H. W. *Biophys. J.* **2001**, *81*, 1475.
(17) Yeaman, M. R.; Yount, N. Y. *Pharmacol. Rev.* **2003**, *55*, 27.
(18) Nguyen, K. T.; Le Clair, S.; Ye, S. J.; Chen, Z. *J. Phys. Chem. B* **2009**, *113*, 12358.
(19) Chen, X.; Chen, Z. *Biochim. Biophys. Acta* **2006**, *1758*, 1257.
(20) Chen, X.; Wang, J.; Boughton, A. P.; Kristalyn, C. B.; Chen, Z. *J. Am. Chem. Soc.* **2007**, *129*, 1420.
(21) Chen, X. Y.; Clarke, M. L.; Wang, J.; Chen, Z. *Int. J. Mod. Phys. B* **2005**, *19*, 691.

(22) Ye, S.; Nguyen, K.; Le Clair, S. V.; Chen, Z. *J. Struct. Biol.* **2009**, *168*, 61.
(23) Ye, S.; Nguyen, K.; Chen, Z. *J. Phys. Chem. B* **2010**, *114*, 3334.
(24) Nguyen, K.; King, J. T.; Chen, Z. *J. Phys. Chem. B* **2010**, *114*, 8291.
(25) Chen, X.; Boughton, A. P.; Tesmer, J. J. G.; Chen, Z. *J. Am. Chem. Soc.* **2007**, *129*, 12658.
(26) Nguyen, K.; Soong, R.; Im, S.; Waskell, L.; Ramamoorthy, A.; Chen, Z. *J. Am. Chem. Soc.* **2010**, *132*, 15112.
(27) Zhuang, X.; Miranda, P. B.; Kim, D.; Shen, Y. R. *Phys. Rev. B* **1999**, *59*, 12633.
(28) Bain, C. D. *J. Chem. Soc., Dalton Trans.* **1995**, *91*, 1281.
(29) Eisenthal, K. B. *Chem. Rev.* **1996**, *96*, 1343.
(30) Wang, J.; Chen, C.; Buck, S. M.; Chen, Z. *J. Phys. Chem. B* **2001**, *105*, 12118.
(31) Wang, J.; Paszti, Z.; Even, M. A.; Chen, Z. *J. Am. Chem. Soc.* **2002**, *124*, 7016.
(32) Scatena, L. F.; Brown, M. G.; Richmond, G. L. *Science* **2001**, *292*, 908.
(33) Chen, Z.; Shen, Y. R.; Somorjai, G. A. *Annu. Rev. Phys. Chem.* **2002**, *53*, 437.
(34) Chen, P.; Kung, K. Y.; Shen, Y. R.; Somorjai, G. A. *Surf. Sci.* **2001**, *494*, 289.
(35) Kim, G.; Gurau, M. C.; Lim, S.-M.; Cremer, P. S. *J. Phys. Chem. B* **2003**, *107*, 1403.
(36) Perry, A.; Neipert, C.; Kasprzyk, C. R.; Green, T.; Space, B.; Moore, P. B. *J. Chem. Phys.* **2005**, *14*, 144705.
(37) Ye, S.; Noda, H.; Nishida, T.; Morita, S.; Osawa, M. *Langmuir* **2004**, *20*, 357.
(38) Gautam, K. S.; Schwab, A. D.; Dhinojwala, A.; Zhang, D.; Dougai, S. M.; Yeganeh, M. S. *Phys. Rev. Lett.* **2000**, *85*, 3854.
(39) Weidner, T.; Breen, N. F.; Li, K.; Drohny, G. P.; Castner, D. G. *Proc. Natl. Acad. Sci. U.S.A.* **2010**, *107*, 13288.
(40) Bordenyuk, A. N.; Jayathilake, H.; Benderskii, A. V. *J. Phys. Chem. B* **2005**, *109*, 15941.
(41) Ma, G.; Liu, D. F.; Allen, H. C. *Langmuir* **2004**, *20*, 11620.
(42) Fitchett, B. A.; Conboy, J. C. *J. Phys. Chem. B* **2004**, *108*, 20255.
(43) Ye, S.; Morita, S.; Li, G.; Noda, H.; Tanaka, M.; Uosaki, K.; Osawa, M. *Macromolecules* **2003**, *36*, 5694.
(44) Kweskin, S. J.; Komvopoulos, K.; Somorjai, G. A. *Langmuir* **2005**, *21*, 3647.
(45) Baldelli, S. *Acc. Chem. Res.* **2008**, *41*, 421.
(46) Chen, Z. *Prog. Polym. Sci.* **2010**, *35*, 1376.
(47) Sharon, M.; Oren, Z.; Shai, Y.; Anglister, J. *Biochemistry* **1999**, *38*, 15305.
(48) Bechinger, B.; Kim, Y.; Chirlian, L. E.; Gesell, J.; Neumann, J. M.; Montal, M.; Tomich, J.; Zasloff, M.; Opella, S. J. *J. Biomol. NMR* **1991**, *1*, 167.
(49) Bechinger, B.; Zasloff, M.; Opella, S. J. *Protein Sci.* **1993**, *2*, 2077.
(50) Porcelli, F.; Buck, B.; Lee, D.; Hallock, K. J.; Ramamoorthy, A.; Veglia, G. *J. Biol. Chem.* **2004**, *279*, 45815.
(51) Henzler Wildman, K. A.; Lee, D.; Ramamoorthy, A. *Biochemistry* **2003**, *42*, 6545.
(52) Henzler-Wildman, K. A.; Martinez, G. V.; Brown, M. F.; Ramamoorthy, A. *Biochemistry* **2004**, *43*, 8459.
(53) Hallock, K. J.; Lee, D.; Omnaas, J.; Mosberg, H. I.; Ramamoorthy, A. *Biophys. J.* **2002**, *83*, 1004.
(54) Hallock, K. J.; Lee, D.; Ramamoorthy, A. *Biophys. J.* **2003**, *84*, 3052.
(55) Giacometti, A.; Ghiselli, R.; Cirioni, O.; Mocchegiani, F.; D'Amato, G.; Orlando, F.; Sisti, V.; Kamysz, W.; Silvestri, C.; Naldoski, P.; Lukasiak, J.; Saba, V.; Scalise, G. *J. Antimicrob. Chemother.* **2004**, *54*, 654.
(56) Almut, M.; Dong-Kuk, L.; Ramamoorthy, A.; Orr, B. G.; Banaszek Holl., M. *Biophys. J.* **2005**, *89*, 4043.
(57) Lindsey, M. G.; Ramamoorthy, A. *Biochim. Biophys. Acta* **2009**, *1788*, 1680.
(58) Ramamoorthy, A.; Thennarasu, S.; Lee, D. K.; Tan, A.; Maloy, L. *Biophys. J.* **2006**, *91*, 206.
(59) Wang, J; Even, M. A.; Chen, X; Schmaier, A. H.; Waite, J. H.; Chen, Z. *J. Am. Chem. Soc.* **2003**, *125*, 9914.
(60) Chen, X.; Wang, J.; Sniadecki, J. J.; Even, M. A.; Chen, Z. *Langmuir* **2005**, *21*, 2662.
(61) Nguyen, K.; Le Clair, S. V.; Ye, S.; Chen, Z. *J. Phys. Chem. B* **2009**, *113*, 12169.
(62) Fuchs, P. C.; Barry, A. L.; Brown, S. D. *Antimicrob. Agents Chemother.* **1998**, *42*, 1213.
(63) Numao, N.; Hirota, Y.; Iwahori, A.; Kidokoro, S.; Sasatsu, M.; Kondo, I.; Itoh, A.; Itoh, E.; Katoh, T.; Shimozono, N.; Yamazaki, A.; Takao, K.; Kobayashi, S. *Biol. Pharm. Bull.* **1999**, *22*, 73.